

Quasinormal modes of charged black holes in Einstein-Maxwell-Weyl gravity*

De-Cheng Zou(邹德成)^{1;1)} Chao Wu(吴超)^{1;2)} Ming Zhang(张明)^{2;3)} Ruihong Yue(岳瑞宏)^{1;4)}

¹Center for Gravitation and Cosmology and College of Physical Science and Technology, Yangzhou University, Yangzhou 225009, China

²Faculty of Science, Xi'an Aeronautical University, Xi'an 710077 China

Abstract: We study quasinormal modes (QNMs) of charged black holes in the Einstein-Maxwell-Weyl (EMW) gravity by adopting the test scalar field perturbation. We find that the imaginary part of QNM frequencies is consistently negative for different angular parameters l , indicating that these modes always decay and are therefore stable. We do not observe a linear relationship between the QNM frequency ω and parameter p for these black holes, as their charge Q causes a nonlinear effect. We evaluate the massive scalar field perturbation in charged black holes and find that random long lived modes (i.e., quasinormal modes) could exist in this spectrum.

Keywords: quasinormal modes, black hole, stability

DOI: 10.1088/1674-1137/44/5/055102

1 Introduction

As is well known, Einstein's general relativity theory is non-renormalizable [1]. One of the most popular methods is to append all possible quadratic curvature invariants to the usual Einstein-Hilbert action [2], despite the existence of ghost-like modes in this theory. These terms constitute the so-called Einstein-Weyl (EW) gravity [3–5], which includes the most general Einstein-Hilbert action with quadratic curvature invariants. Subsequently, the non-Schwarzschild black hole (NSBH) solutions were recovered in four dimensional spacetime [3, 4], where they also satisfy the condition of the Ricci scalar ($R = 0$). Since the Ricci scalar R does not vanish in higher dimensional ($n > 4$) spacetime, Lü et al. found only the perturbed numerical solutions in the EW gravity [6]. Employing the continued fraction method, Kokkotas et al. constructed a numerical black hole solution in an analytical form [7], and its Hawking radiation was discussed in Ref. [8]. Furthermore, some new solutions were derived in anti-de Sitter (AdS) spacetime [9, 10].

Recently, charged black holes were derived in Refs. [11–13] by applying the four dimensional EW theory coupled with an electromagnetic field. According to the 'seed' solution, these solutions can be divided into two

groups in the Einstein-Maxwell-Weyl (EMW) theory. Group **I** solutions correspond to the charged extension of the higher derivative curvature for a Schwarzschild black hole. In Group **II**, the solutions are constructed from the charged generalization of the NSBH solution. The thermodynamic properties of these charged black holes were investigated in Ref. [13].

The quasinormal modes (QNMs) of a black hole have been a hot research topic for decades. The concept of QNMs was introduced in 1957 by the work of Regge and Wheeler, who investigated the stability of black holes under small perturbations [14]. The study of QNMs is beneficial to the understanding of the structure of black hole spacetimes and could play an important role in the detection of gravitational waves and some fundamental symmetries for the gauge/gravity duality [15, 16]. To date, QNMs have been calculated either by Einstein's general relativity theory coupled with Maxwell theory [17–19] or nonlinear electrodynamics [20–24], or by modified gravities [25–28]. The analysis of QNMs of the non-Schwarzschild black holes was performed in the EW gravity [29, 30], where the linear relation between QNM frequencies and the parameter $p = \frac{r_0}{\sqrt{2}\alpha}$ was recovered. Inspired by these results, we evaluate the effect of the charge Q on the QNMs and the stability of charged black holes in the

Received 18 September 2019, Revised 19 November 2019, Published online 2 March 2020

* Supported by Natural Science Foundation of China (11605152, 11675139, 51802247)

1) E-mail: dczou@yzu.edu.cn

2) E-mail: wc130330@163.com

3) E-mail: mingzhang0807@126.com

4) E-mail: rhyue@yzu.edu.cn

©2020 Chinese Physical Society and the Institute of High Energy Physics of the Chinese Academy of Sciences and the Institute of Modern Physics of the Chinese Academy of Sciences and IOP Publishing Ltd

Einstein-Maxwell-Weyl gravity. We will calculate the QNMs by considering test massless and massive scalar field perturbations on the charged black holes, respectively.

This paper is constructed as follows. We first review charged black hole solutions with an increase of charge Q in the EMW gravity in Section 2. Then, we provide a detailed discussion of QNM frequencies under test scalar field perturbations, including massless and massive scalar fields in Section 3. Finally, we provide concluding remarks in the fourth section.

2 Charged black holes in EMW gravity

The action of the Einstein-Weyl gravity, combined with the electromagnetic field, is given by [12, 13]

$$\mathcal{I} = \frac{1}{16\pi G} \int d^4x \sqrt{-g} [R - \alpha C_{\mu\nu\rho\sigma} C^{\mu\nu\rho\sigma} - \kappa F_{\mu\nu} F^{\mu\nu}], \quad (1)$$

where $F_{\mu\nu} = \nabla_\mu A_\nu - \nabla_\nu A_\mu$ is the electromagnetic tensor. Here, $C_{\mu\nu\rho\sigma}$ is the Weyl tensor and the trace-free part of the Riemann tensor with the form [31, 32]

$$C_{\mu\nu\rho\sigma} = R_{\mu\nu\rho\sigma} - (g_{\mu[\rho} R_{\sigma]\nu} - g_{\nu[\rho} R_{\sigma]\mu}) + \frac{1}{3} R g_{\mu[\rho} R_{\sigma]\nu},$$

where the part within brackets surrounding the indices refers to the anti-symmetric part. To date, various attempts have been made to formulate the Weyl curvature hypothesis in a rigorous way. The simplest choice of a scalar constructed from the Weyl tensor is $C_{\mu\nu\rho\sigma} C^{\mu\nu\rho\sigma}$ from Eq. (1).

The equations of motion are obtained as [12, 13]

$$R_{\mu\nu} - \frac{1}{2} g_{\mu\nu} R - 4\alpha B_{\mu\nu} - 2\kappa T_{\mu\nu} = 0, \quad \nabla_\mu F^{\mu\nu} = 0, \quad (2)$$

where $B_{\mu\nu}$ is the trace-free Bach tensor, and $T_{\mu\nu}$ is energy-momentum tensor of the Maxwell field

$$\begin{aligned} B_{\mu\nu} &= \left(\nabla^\rho \nabla^\sigma + \frac{1}{2} R^{\rho\sigma} \right) C_{\mu\nu\rho\sigma}, \\ T_{\mu\nu} &= F_{\alpha\mu} F_{\nu}^{\alpha} - \frac{1}{4} g_{\mu\nu} F_{\alpha\beta} F^{\alpha\beta}. \end{aligned} \quad (3)$$

We choose the metric ansatz

$$ds^2 = -N(r)e^{-2\delta(r)} dt^2 + \frac{1}{N(r)} dr^2 + r^2 (d\theta^2 + \sin^2\theta d\varphi^2) \quad (4)$$

with a metric function $N(r)$ equal to $1 - 2m(r)/r$. We constructed numerical charged black hole solutions with $\alpha = \frac{1}{2}$ and $\kappa = 1$ [13], according to two neutral scenarios: the Schwarzschild (SBH) and non-Schwarzschild black hole (NSBH) within the bound of $0.363 < r_0 < 1.143$ in the EW theory. Fig. 1 presents the relation between the mass M and Hawking temperature T for SBH and NSBH scenarios, where both neutral solutions coalesce at $T \approx 0.091$ ($r_0 \approx 0.876$). Taking Group I (Fig. 1(a)) as an example, charged black holes were constructed from the Schwarzschild black hole ($Q=0$) by increasing the charge Q while maintaining the same horizon radius r_0 . In particular, new charged black holes on both sides of the coalescent point exhibit different properties: as the charge Q increases, their mass becomes larger (smaller) depending on the temperature decrease (increase) on the left (right) hand side. A similar phenomenon is observed in Group II, as shown in Fig. 1(b).

3 Quasinormal modes for test scalar field

In this section, we consider the test massive scalar field ψ propagating on charged black holes, which obeys the Klein-Gordon equation

$$(\square - \mu^2)\psi = 0, \quad (5)$$

where μ is the mass of the scalar field, and ψ can be separated into spherical harmonics, temporal, and radial

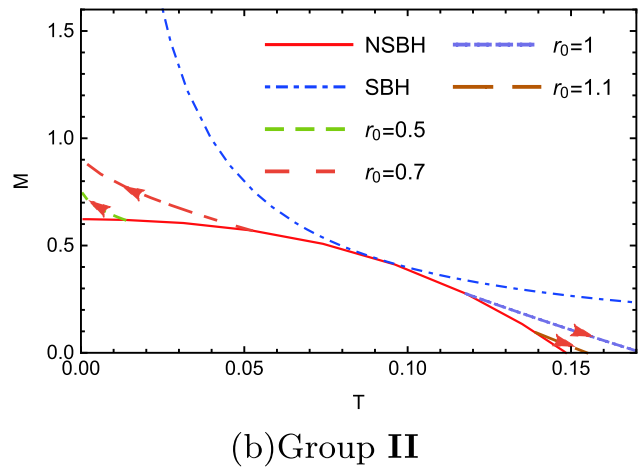
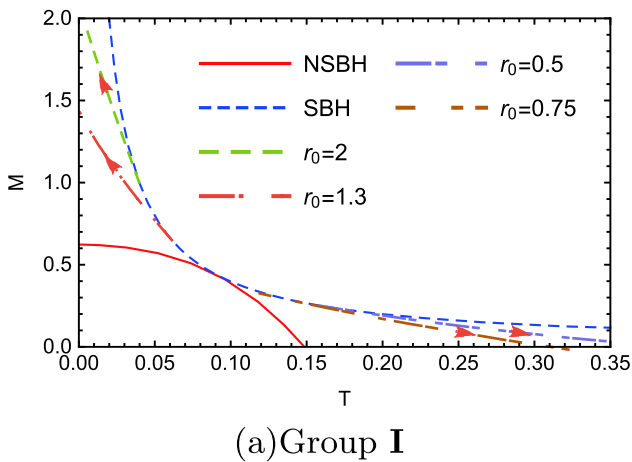


Fig. 1. (color online) Mass M versus temperature T for Schwarzschild (SBH), non-Schwarzschild (NSBH), and charged black holes for Group I (a) and Group II (b). The arrow denotes the increase in charge Q .

components

$$\psi(t, r, \theta, \phi) = \sum_{lm} \frac{1}{r} \Psi_l(r) Y_{lm}(\theta, \phi) e^{-i\omega t}, \quad (6)$$

where $Y_{lm}(\theta, \phi)$ is a usual spherical harmonic, and l is the angular harmonic index.

Substituting Eqs. (4) and (6) into Eq. (5), we obtain the radial perturbed Schrödinger equation

$$(\partial_{r_*}^2 + \omega^2 - V_l(r)) \Psi_l(r) = 0, \quad (7)$$

where the effective potential is given as

$$V_l = \frac{l(l+1)Ne^{-2\delta}}{r^2} + \frac{Ne^{-2\delta}(N' - N\delta')}{r} + \mu^2 Ne^{-2\delta} \quad (8)$$

and the tortoise coordinate r_* is adopted as

$$\frac{dr_*}{dr} = \frac{1}{Ne^{-\delta}}. \quad (9)$$

3.1 Quasinormal modes for massless scalar field

We consider the massless scalar field perturbation

($\mu = 0$) in these charged black holes for Groups I and II. First, we choose appropriate boundary conditions. The respective boundary conditions at the black hole horizon and spatial infinity are

$$\Psi_l(r) \sim \begin{cases} e^{-i\omega r_*} \sim (r-r_0)^{-\frac{i\omega}{4\pi r}} & r \rightarrow r_0 (r_* \rightarrow -\infty) \\ e^{i\omega r_*} \sim e^{-i\omega r} r^{2M i \omega} & r \rightarrow \infty (r_* \rightarrow \infty), \end{cases} \quad (10)$$

To derive these QN modes ω , we employ the shooting method [33-35]. With the initial condition given by Eq. (10) at the event horizon r_0 , we solve the perturbed Eq. (7) numerically for each ω using the *Wolfram Mathematica*® built-in function `NDSolve` for $r_0 \leq r \leq r_f$, where $r_f \gg r_0$. This solution must also satisfy the boundary condition in Eq. (10) at spatial infinity, if ω is the quasinormal frequency.

In the Tables 1-4, we present QNM frequencies (real and imaginary parts) for these charged black holes in Groups I and II. The QNM frequencies (for $l = 0$ and 1) of these neutral black holes (SBH and NSBH) are displayed in the first row of Tables 1-4. In the case of

Table 1. QNM frequencies of black holes within region of $r_0 < 0.876$ in Group I.

Q	$r_0 = 0.5$		$r_0 = 0.75$	
	$\omega(l=0)$	$\omega(l=1)$	$\omega(l=0)$	$\omega(l=1)$
0	0.4420-0.4196i	1.1716-0.3908i	0.2947-0.2797i	0.7810-0.2605i
0.02	0.445730-0.419802i	1.17219-0.39126i	0.29504-0.284839i	0.781750-0.262508i
0.06	0.447649-0.423259i	1.17636-0.394006i	0.300096-0.291943i	0.768417-0.266851i
0.1	0.451833-0.431002i	1.18541-0.399437i	0.305035-0.307715i	0.795061-0.269681i
0.14	0.458975-0.443435i	1.19959-0.408586i	0.310574-0.309508i	0.806376-0.275657i
0.18	0.465102-0.456727i	1.21463-0.420002i	0.315876-0.317400i	0.820854-0.281226i
0.22	0.467173-0.461698i	1.23312-0.434605i	0.318256-0.328687i	0.825449-0.304661i
0.26	0.481790-0.486744i	1.25409-0.445270i	0.321404-0.342171i	0.830678-0.326003i
0.30	0.512190-0.519842i	1.27810-0.477936i	0.324608-0.355701i	0.834912-0.334916i
0.33	0.522566-0.532159i	1.29662-0.490691i	0.330838-0.369421i	0.838476-0.351239i

Table 2. QNM frequencies of black holes within region of $r_0 > 0.876$ in Group I.

Q	$r_0 = 1.3$		$r_0 = 2$	
	$\omega(l=0)$	$\omega(l=1)$	$\omega(l=0)$	$\omega(l=1)$
0	0.1700-0.1614i	0.4506-0.1503i	0.1105-0.1049i	0.2929-0.0977i
0.02	0.169935-0.160131i	0.449981-0.149923i	0.110434-0.104754i	0.292409-0.0975053i
0.06	0.169604-0.158960i	0.449018-0.149611i	0.110072-0.104079i	0.290913-0.0960668i
0.1	0.169109-0.157354i	0.448207-0.148787i	0.108803-0.101841i	0.287647-0.0937670i
0.14	0.168720-0.155810i	0.447165-0.147679i	0.106439-0.098191i	0.283246-0.0906137i
0.18	0.168023-0.153998i	0.443449-0.145653i	0.103804-0.0933381i	0.278075-0.0869171i
0.22	0.166891-0.151193i	0.441312-0.143235i	0.101889-0.0875931i	0.272255-0.0830565i
0.26	0.166014-0.148333i	0.437092-0.140916i	0.100331-0.0820946i	0.266262-0.0790222i
0.30	0.165430-0.144852i	0.432538-0.137778i	0.098978-0.0771625i	0.259892-0.0749341i
0.33	0.164395-0.143688i	0.429952-0.135908i	0.098060-0.0736714i	0.254996-0.0719146i

Table 3. QNM frequencies of black holes within region of $r_0 < 0.876$ in Group II.

Q	$r_0 = 0.5$		$r_0 = 0.7$	
	$\omega(l=0)$	$\omega(l=1)$	$\omega(l=0)$	$\omega(l=1)$
0	0.1920-0.05801i	0.5650-0.1168i	0.2484-0.1550i	0.5574-0.4347i
0.02	0.191974-0.0578165i	0.563943-0.115416i	0.247626-0.15488i	0.556522-0.433647i
0.06	0.191900-0.0575649i	0.561869-0.114350i	0.245508-0.153018i	0.551806-0.407181i
0.1	0.191801-0.0572173i	0.556545-0.112453i	0.242262-0.150052i	0.550735-0.410594i
0.12	0.191707-0.0569421i	0.553771-0.111982i	0.240109-0.148196i	0.548074-0.403119i
0.155	0.191457-0.0563484i	0.547261-0.109390i	0.235633-0.144682i	0.542076-0.386617i
0.185	0.191279-0.0559977i	0.543921-0.104531i	0.231188-0.141623i	0.536208-0.369774i
0.215	0.190982-0.0555578i	0.534453-0.100874i	0.226304-0.138735i	0.530038-0.353073i
0.25	0.188420-0.0548792i	0.521852-0.094748i	0.220221-0.135954i	0.518341-0.344284i
0.29	0.185355-0.0536175i	0.508852-0.087635i	0.213025-0.133582i	0.508015-0.333045i

Table 4. QNM frequencies of black holes within region of $r_0 > 0.876$ in Group II.

Q	$r_0 = 1$		$r_0 = 1.1$	
	$\omega(l=0)$	$\omega(l=1)$	$\omega(l=0)$	$\omega(l=1)$
0	0.2490-0.3900i	0.6920-0.2920i	0.2967-0.4970i	0.7764-0.3774i
0.02	0.248326-0.390859i	0.697313-0.292519i	0.298359-0.497294i	0.78196-0.3774330i
0.055	0.249730-0.398086i	0.699694-0.294816i	0.300096-0.497879i	0.786675-0.377930i
0.09	0.251139-0.403061i	0.706433-0.300164i	0.303839-0.507651i	0.795747-0.387478i
0.125	0.258110-0.418834i	0.713570-0.308565i	0.313144-0.495390i	0.795217-0.390079i
0.16	0.257806-0.426266i	0.722897-0.314524i	0.315173-0.529731i	0.816878-0.410238i
0.195	0.262761-0.434169i	0.731343-0.322654i	0.322461-0.538773i	0.827657-0.422568i
0.23	0.266851-0.445229i	0.740003-0.332937i	0.328884-0.559389i	0.842650-0.437051i
0.28	0.279679-0.465540i	0.749440-0.341363i	0.341379-0.571647i	0.860521-0.459423i

$Q \rightarrow 0$, the action presented in Eq. (1) becomes neutral [3, 4], recovering the Schwarzschild and non-Schwarzschild solutions in four dimensional spacetime. The fundamental QNM frequencies under a massless scalar field perturbation on the SBH background are given in Refs. [36, 37]. QNM frequencies (for $l = 0$ and 1) of the NSBH with a horizon radius $r_0 > 0.876$ are provided in Refs. [29, 30]. However, for the NSBH with $r_0 < 0.876$, there is a discrepancy between QNM frequencies and data obtained from the relation expression $p \sim \omega$ in Ref. [30]. This is probably because this expression, derived in the bound $0.876 < r_0 < 1.143$, is not valid in the region of $0.363 < r_0 < 0.876$ for the NSBH in the EW gravity.

For charged black holes, the imaginary parts are always negative, indicating that these modes always decay and are therefore stable. Moreover, for the charged black holes with $r_0 = 0.5$ and 0.75 in Group I, the absolute values of the imaginary part ($|\omega_i|$) and real part (ω_r) of QNM frequencies ($l = 0, 1$) both increase with increasing of Q (see Table 1 and Fig. 2(a)). In contrast, the correspond-

ing values of $|\omega_i|$ and ω_r of QNM frequencies for charged black holes with $r_0 = 1.3$ and 2 in Group I both decrease with increasing of Q (see Table 2 and Fig. 2(b)). Similarly, QNM frequencies of these charged black holes in Group II, located each side of the coalescent point $T \approx 0.091 (r_0 \approx 0.876)$, exhibit different trends from the ones given in Tables 3, 4 and Fig. 3. This is because the mass M and temperature T of these charged black holes affect the boundary conditions of the test scalar field $\Psi_l(r)$ given in Eq. (10). However, based on the free energies (Fig. 7 in Ref. [13]) and QNM frequencies of these charged and neutral black holes [Figs. 2 and 3], the correlation between thermodynamic phase transitions and dynamical stabilities fails.

Notably, the study of Ref. [30] asserted that QNM frequencies ω are linearly dependent on $p = \frac{r_0}{\sqrt{2\alpha}}$ for NSBH in the EW gravity. Following a similar path, we assume $\alpha = 1/2$ and a fixed charge Q , and subsequently consider QNMs of the new charged black holes with a different horizon radius r_0 (here, we do not show new nu-

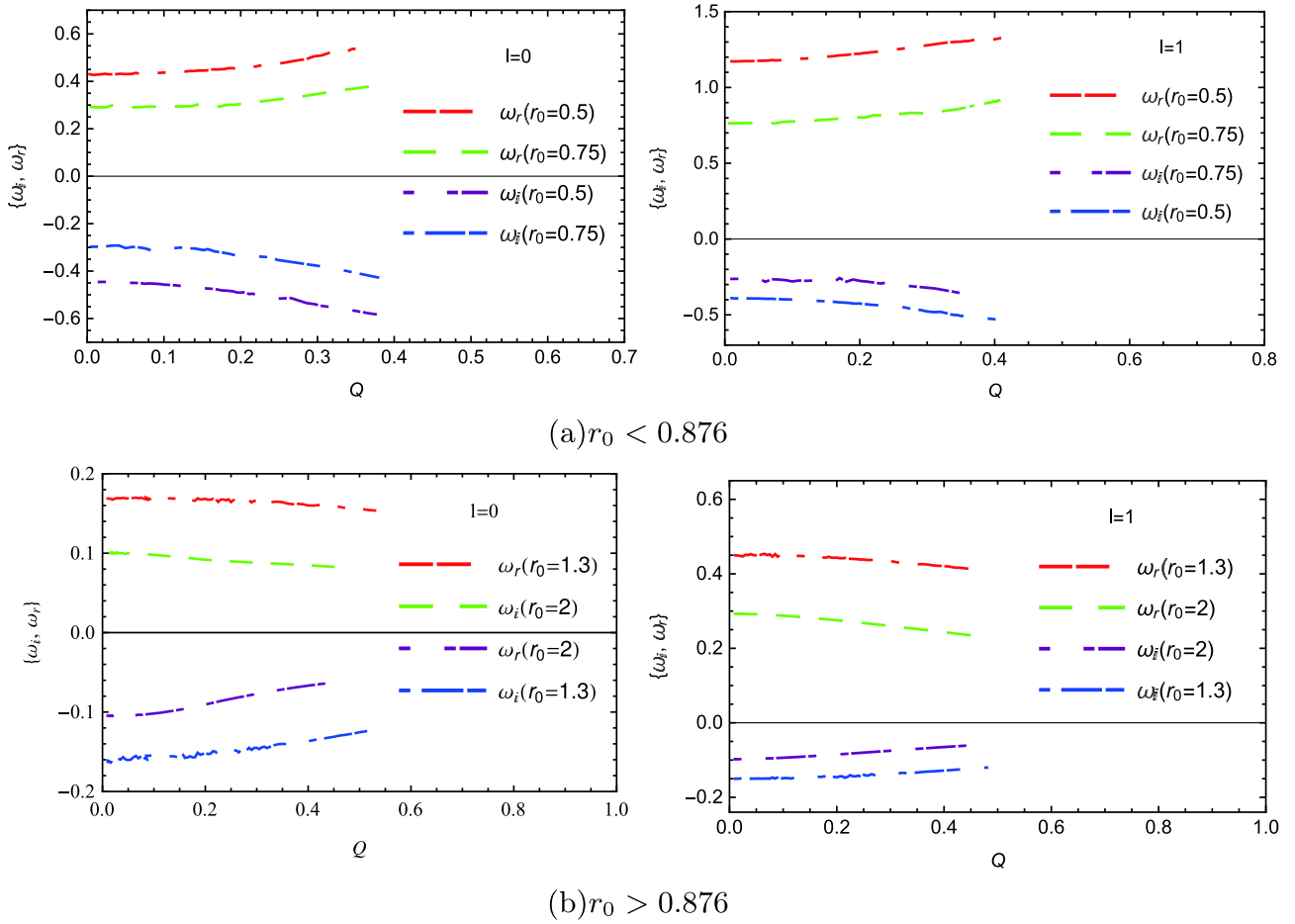


Fig. 2. (color online) Dependence of fundamental QNM frequencies of charged black hole on charge Q with fixed horizon radius in Group I.

merical solutions) for various multipole numbers l , assuming $p = \frac{r_0}{\sqrt{2\alpha}} = r_0$. According to QNM frequencies of charged black holes with $r_0 = p = 0.5$ in Group I and $r_0 = p = 0.7$ in Group II, these new QNM frequencies are expressed as a function of p in Table 5 and Figs. 4 and 5. In comparison with QNMs of charged black holes with $p = r_0 = 0.5$, the new charged black holes with different values of $p = r_0 > 0.5$ exhibit lower real frequencies and a lower damping rate. Moreover, the tendency of the imaginary part of QNM frequencies for $l = 1$ changes, as shown in Fig. 5(b). Finally, we do not observe the strict linear relation between ω and p , as the charge Q causes a nonlinear effect on the frequency for these charged black holes in the EMW gravity.

3.2 Quasinormal modes for massive scalar field

We consider how the behavior of QNMs changes depending on the massive scalar field $\mu \neq 0$. Under the massive scalar field perturbation, the boundary conditions are different from those in the massless case. From the radial perturbed Schrödinger Eq. (7), the respective ingoing boundary conditions at the black hole event hori-

zon and outgoing boundary conditions at spatial infinity are obtained as

$$\Psi_l(r) \sim \begin{cases} e^{-i\omega r_*} \sim (r-r_0)^{-\frac{i\omega}{4\pi r}}, & r \rightarrow r_0 \\ e^{i(\mu^2 - \omega^2)^{1/2} r_*} \sim r m e^{-(\mu^2 - \omega^2)^{1/2} r} r^{-2M(\mu^2 - \omega^2)^{1/2}}, & r \rightarrow \infty \end{cases} \quad (11)$$

We take as an example the charged black holes with $r_0 = 0.5$ and $Q = 0.1$ in Group I. The QNM frequencies as a function of mass μ are shown in Fig. 6 [38]. For the angular parameter $l = 0$, the real part of the QNM frequencies becomes larger, while the imaginary part decreases with increasing mass μ . This indicates that massive modes are scattered more slowly than massless modes. Moreover, these oscillations could become undamped, i.e., $\omega_i = 0$, under certain conditions, causing the appearance of so-called quasinormal modes. This phenomenon emerged for the massive scalar field perturbation in the NSBH background in EW gravity [30] and the charged field perturbation in the RN black hole [39, 40, 41]. Nevertheless, these quasinormal modes disappear for $l = 1$ in the EMW gravity.

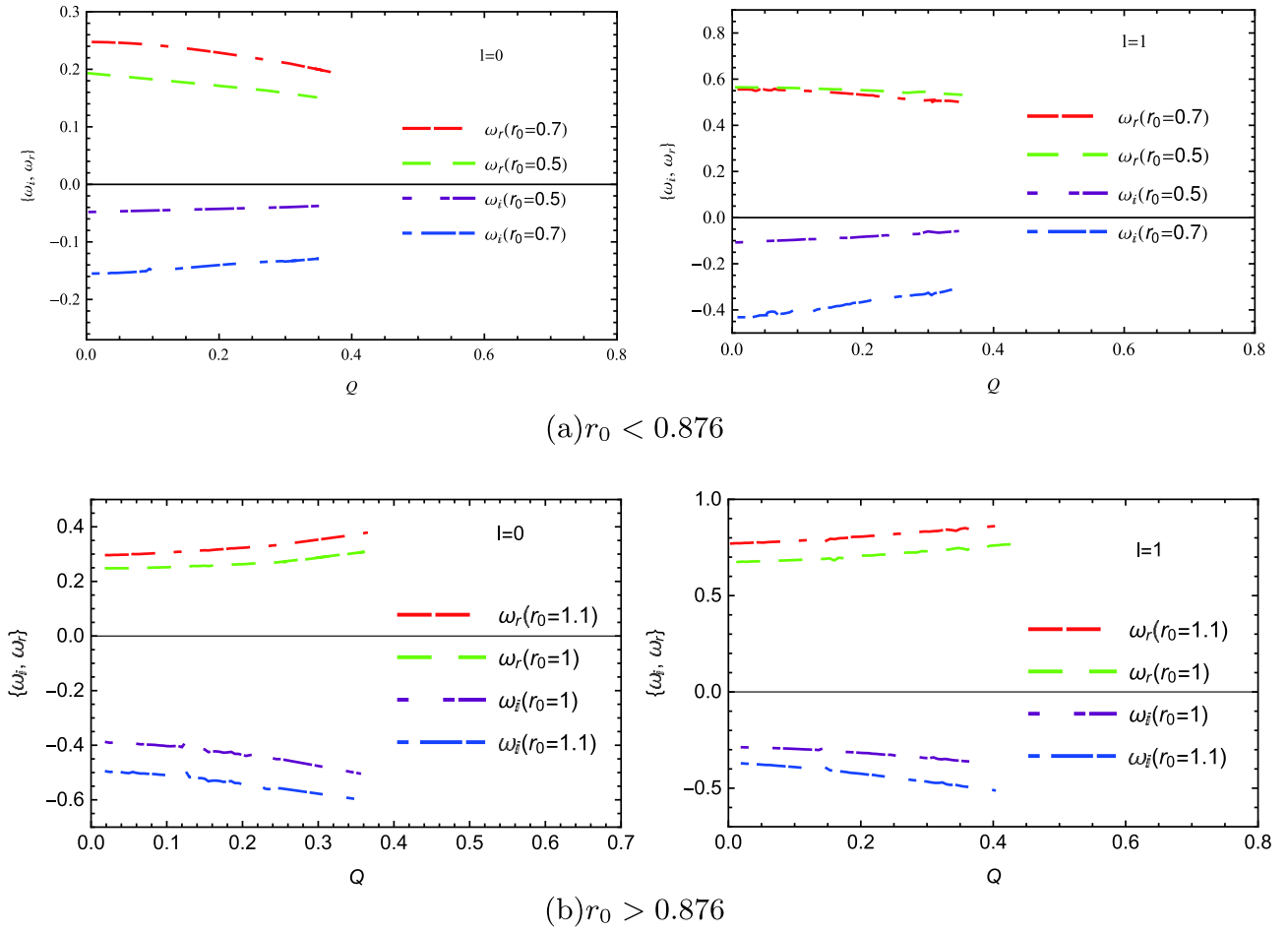


Fig. 3. (color online) Dependence of fundamental QNM frequencies of charged black hole on charge Q with fixed horizon radius in Group II.

Table 5. Dependence of QNM frequencies of charged black hole on parameter p with fixed $Q = 0.1$ in Groups I and II.

Group I			Group II		
p	$\omega(l=0)$	$\omega(l=1)$	p	$\omega(l=0)$	$\omega(l=1)$
0.5	0.451303-0.428182i	1.185030-0.399112i	0.7	0.242462-0.150258i	0.551352-0.409716i
0.54	0.423578-0.399711i	1.099260-0.366381i	0.685	0.242485-0.150641i	0.560200-0.387280i
0.58	0.386467-0.369919i	1.019980-0.348577i	0.665	0.242862-0.151787i	0.568930-0.372865i
0.63	0.356692-0.342205i	0.939253-0.320923i	0.65	0.243282-0.153298i	0.574191-0.367385i
0.68	0.329482-0.312415i	0.862011-0.294039i	0.64	0.243481-0.155328i	0.583836-0.360624i
0.72	0.313943-0.302641i	0.823348-0.279923i	0.62	0.244227-0.162025i	0.601820-0.359452i
0.75	0.300831-0.297926i	0.797623-0.271460i	0.6	0.246600-0.169481i	0.60298-0.346543i

4 Conclusions and discussions

Applying the Einstein-Maxwell-Weyl theory, we investigated QNMs and the stability of charged black holes under the test scalar field perturbation. With an increase in the charge Q , QNM frequencies are depicted by larger (smaller) real oscillations and higher (lower) damping rates, than those for the neutral branches at the same side

of the coalescent point $T \approx 0.091$ ($r_0 \approx 0.876$), in both Groups I and II. Moreover, these phenomena are reflected by the behaviors of the thermodynamic quantities M and T . Furthermore, the linear dependence of the QNM frequency on the parameter p for NSBH in the EW gravity does not manifest for the new charged black holes in the EMW gravity, as the charge Q causes a nonlinear effect on QNM frequencies. Furthermore, we discussed the

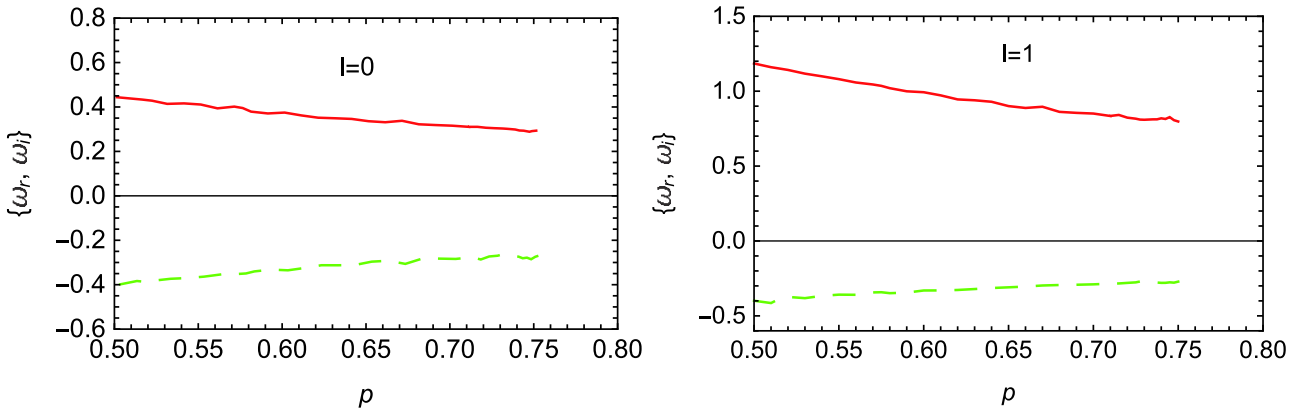


Fig. 4. (color online) Dependence of QNM frequencies of charged black hole on parameter p with $Q = 0.1$ starting from $Q = 0.1$ and $p = r_0 = 0.5$ in Group I. Solid and dashed lines denote the real and imaginary parts of QNM frequencies, respectively.

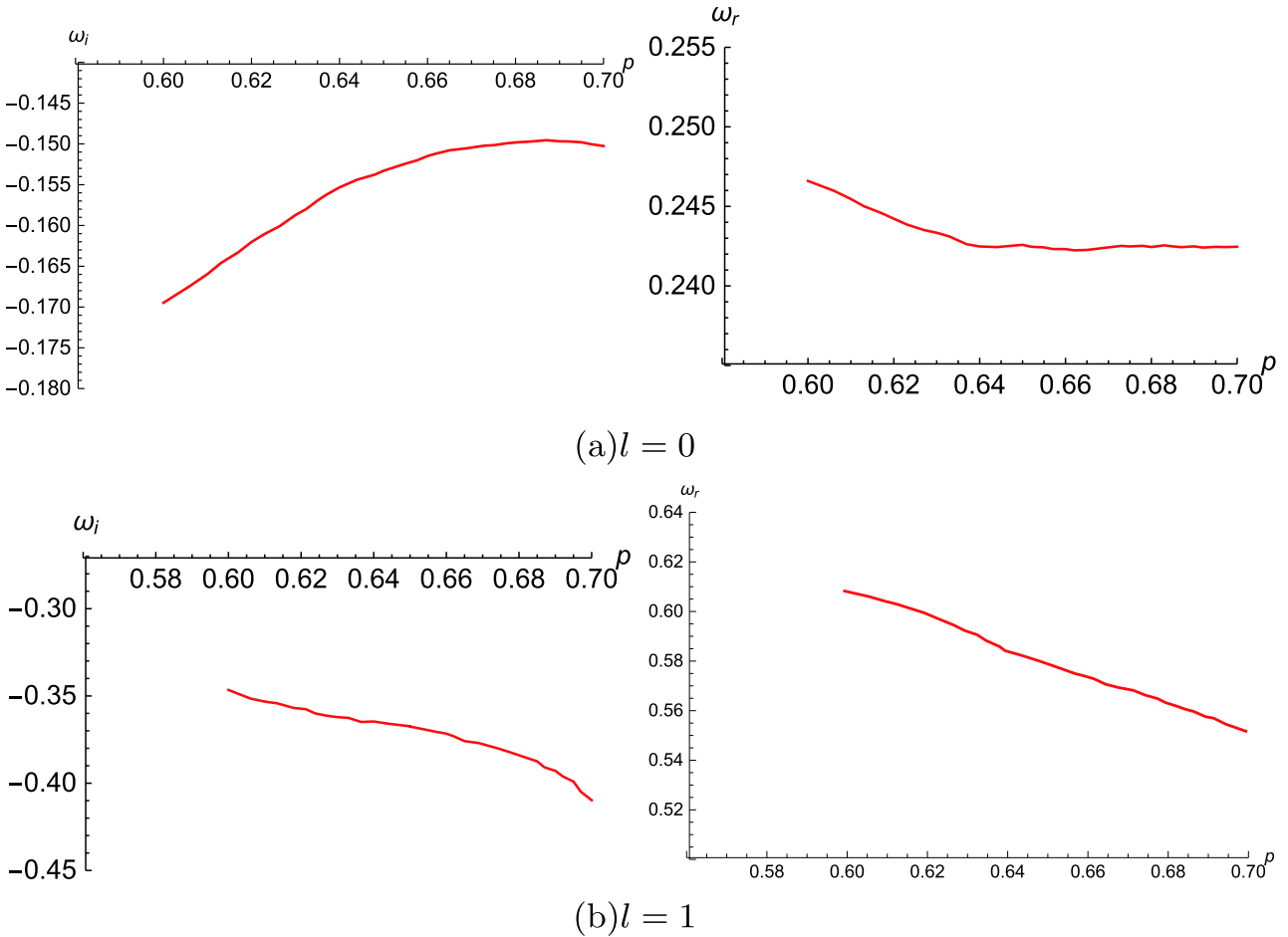


Fig. 5. (color online) Dependence of QNM frequencies of charged black hole on parameter p with $Q = 0.1$ starting from $Q = 0.1$ and $p = r_0 = 0.7$ in Group II.

case of a massive scalar field perturbation, where undamped oscillations occur for sufficiently large masses.

Recently, (anti-) de Sitter charged black hole solutions in the EMW gravity were presented [11]. Because

of the dual conformal field theory, QNM frequencies of AdS black holes have a direct interpretation [42, 43]. Therefore, it would be interesting to consider QNMs and the stability of charged AdS black holes in the EMW gravity.

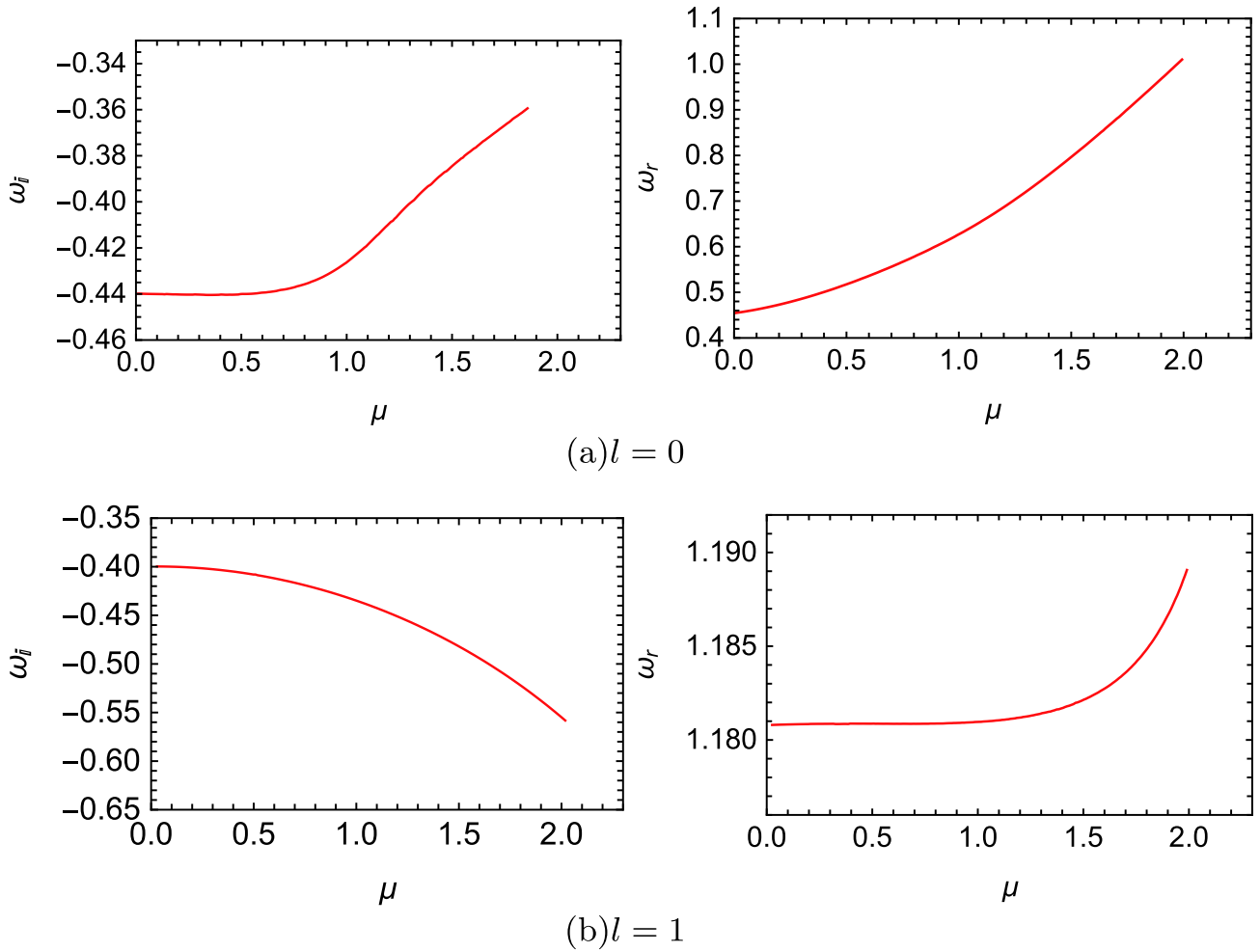


Fig. 6. (color online) Dependence of QNM frequencies of charged black hole on mass μ with $r_0 = 0.5$ and $Q = 0.1$ in Group I on the mass.

References

- 1 G. 't Hooft and M. J. G. Veltman, *Ann. Inst. H. Poincaré Phys. Theor. A*, **20**: 69 (1974)
- 2 K. S. Stelle, *Phys. Rev. D*, **16**: 953 (1977)
- 3 H. Lü, A. Perkins, C. N. Pope, and K. S. Stelle, *Phys. Rev. Lett.*, **114**: 171601 (2015)
- 4 H. Lü, A. Perkins, C. N. Pope *et al.*, *Phys. Rev. D*, **92**: 124019 (2015)
- 5 B. Holdom and J. Ren, *Phys. Rev. D*, **95**: 084034 (2017)
- 6 H. Lü, A. Perkins, C. N. Pope, and K. S. Stelle, *Phys. Rev. D*, **96**: 046006 (2017)
- 7 K. Kokkotas, R. A. Konoplya, and A. Zhidenko, *Phys. Rev. D*, **96**: 064007 (2017)
- 8 R. A. Konoplya and A. F. Zinhailo, arXiv:1904.05341 [gr-qc]
- 9 J. Podolsky, R. Svarc, V. Pravda *et al.*, *Phys. Rev. D*, **98**: 021502 (2018)
- 10 R. Svarc, J. Podolsky, V. Pravda *et al.*, *Phys. Rev. Lett.*, **121**: 231104 (2018)
- 11 K. Lin, W. L. Qian, A. B. Pavan *et al.*, *EPL*, **114**(6): 60006 (2016)
- 12 K. Lin, A. B. Pavan, G. Flores-Hidalgo *et al.*, *Braz. J. Phys.*, **47**: 419 (2017)
- 13 C. Wu, D. C. Zou, and M. Zhang, arXiv:1904.10193 [gr-qc]
- 14 T. Regge and J. A. Wheeler, *Phys. Rev.*, **108**: 1063 (1957)
- 15 S. Chandrasekhar, OXFORD, UK: CLARENDON (1985) 646 P
- 16 E. Berti, V. Cardoso, and A. O. Starinets, *Class. Quant. Grav.*, **26**: 163001 (2009), arXiv:0905.2975[gr-qc]
- 17 R. A. Konoplya, *Gen. Rel. Grav.*, **34**: 329 (2002), arXiv:[gr-qc/0109096]
- 18 H. Onozawa, T. Mishima, T. Okamura *et al.*, *Phys. Rev. D*, **53**: 7033 (1996), arXiv:[gr-qc/9603021]
- 19 O. P. F. Piedra and J. de Oliveira, *Class. Quant. Grav.*, **28**: 085003 (2011), arXiv:1006.3802[gr-qc]
- 20 G. Panotopoulos, *Gen. Rel. Grav.*, **50**(6): 59 (2018), arXiv:1805.04743[hep-th]
- 21 ÁRincón and G. Panotopoulos, *Phys. Rev. D*, **97**(2): 024027 (2018), arXiv:1801.03248[hep-th]
- 22 G. Panotopoulos and Á Rincón, *Int. J. Mod. Phys. D*, **27**(03): 1850034 (2017), arXiv:1711.04146[hep-th]
- 23 G. Panotopoulos and Á Rincón, *Eur. Phys. J. Plus*, **134**(6): 300 (2019), arXiv:1904.10847[gr-qc]
- 24 K. Destounis, G. Panotopoulos, and Á Rincón, *Eur. Phys. J. C*, **78**(2): 139 (2018), arXiv:1801.08955[gr-qc]
- 25 D. Yoshida and J. Soda, *Phys. Rev. D*, **93**(4): 044024 (2016), arXiv:1512.05865[gr-qc]
- 26 R. Li and J. R. Ren, *Phys. Rev. D*, **83**: 064024 (2011), arXiv:1008.3239[hep-th]
- 27 S. Chen and J. Jing, *Phys. Lett. B*, **687**: 124 (2010), arXiv:0905.1409[gr-qc]
- 28 R. Konoplya, *Phys. Rev. D*, **71**: 024038 (2005), arXiv:[hep-th/0410057]

- 29 Y. F. Cai, G. Cheng, J. Liu *et al.*, *JHEP*, **1601**: 108 (2016)
- 30 A. F. Zinhailo, *Eur. Phys. J. C*, **78**(12): 992 (2018) [*Eur. Phys. J.*, **78**: 992 (2018)]
- 31 S. Chen, S. Wang, Y. Huang *et al.*, *Phys. Rev. D*, **95**(10): 104017 (2017), arXiv:1611.08783[gr-qc]
- 32 T. A. Malik and R. Lopez-Mobilia, arXiv:1910.07598 [gr-qc]
- 33 R. A. Konoplya and A. Zhidenko, *Rev. Mod. Phys.*, **83**: 793 (2011), arXiv:1102.4014 [gr-qc]
- 34 P. A. Gonzalez, R. A. Konoplya, and Y. Vasquez, *Phys. Rev. D*, **95**(12): 124012 (2017), arXiv:1703.06215[gr-qc]
- 35 R. A. Konoplya and A. Zhidenko, *JHEP*, **1709**: 139 (2017), arXiv:1705.07732[hep-th]
- 36 S. Iyer, *Phys. Rev. D*, **35**: 3632 (1987)
- 37 R. A. Konoplya, *Phys. Rev. D*, **68**: 024018 (2003), arXiv:[gr-qc/0303052]
- 38 We do not present the QNM frequencies of charged black holes under the massive scalar field perturbation in a table, because there are clear trend of change for these QNM frequencies
- 39 A. Ohashi and M. a. Sakagami, *Class. Quant. Grav.*, **21**: 3973 (2004)
- 40 S. Hod, *Phys. Lett. B*, **761**: 53 (2016)
- 41 S. Hod, *Eur. Phys. J. C*, **77**(5): 351 (2017)
- 42 V. Cardoso, o J. C. Dias, G. S. Hartnet *et al.*, *JHEP*, **1404**: 183 (2014)
- 43 V. Cardoso, R. Konoplya, and J. P. S. Lemos, *Phys. Rev. D*, **68**: 044024 (2003)